Resonance Raman and DFT Studies of Tetra-*tert*-butyl Porphine: Assignment of Strongly Enhanced Distortion Modes in a Ruffled Porphyrin

Roma E. Oakes, Stephen J. Spence, and Steven E. J. Bell*

School of Chemistry, Queen's University, Belfast BT9 5AG, Northern Ireland

Received: December 17, 2002; In Final Form: February 20, 2003

The free-base form of tetra-*tert*-butyl porphine (TtBP), which has extremely bulky *meso* substituents, is severely distorted from planarity, with a ruffling angle of 65.5°. The resonance Raman spectrum of TtBP ($\lambda_{ex} = 457.9$ nm) and its d_2, d_8, and d_{10} isotopomers have been recorded, and while the spectra show high-frequency bands similar to those observed for planar *meso*-substituted porphyrins, there are several additional intense bands in the low-frequency region. Density functional calculations at the B3-LYP/6-31G(d) level were carried out for all four isotopomers, and calculated frequencies were scaled using a single factor of 0.98. The single factor scaling approach was validated on free base porphine where the RMS error was found to be 14.9 cm^{-1}. All the assigned bands in the high-frequency (>1000 cm^{-1}) region of TtBP were found to be due to vibrations similar in character to the in-plane skeletal modes of conventional planar porphyrins. In the low-frequency region, two of the bands, assigned as ν_8 (ca. 330 cm^{-1}) and ν_{16} (ca. 540 cm^{-1}), are also found in planar porphyrins such as tetra-phenyl porphine (TPP) and tetra-*iso*-propyl porphine (IPP). Of the remaining three very strong bands, the lowest frequency band was assigned as γ_{12} (pyr swivel, obsd 415 cm^{-1}, calcd 407 cm^{-1} in d_0). The next band, observed at 589 cm^{-1} in the d_0 compound (calcd 583 cm^{-1}), was assigned as a mode whose composition is a mixture of modes that were previously labeled γ_{13} ($\gamma(C_mC_aH_mC_a)$) and γ_{11} (pyr $fold_{asym}$) in NiOEP. The final strong band, observed at 744 cm^{-1} (calcd 746 cm^{-1}), was assigned to a mode whose composition is again a mixture of $\gamma_{11}$and γ_{13}, although here it is γ_{11} rather than γ_{13} which predominates. These bands have characters and positions similar to those of three of the four porphyrin ring-based, weak bands that have previously been observed for NiTPP. In addition there are several weaker bands in the TtBP spectra that are also "out-of-plane" vibrations. Two of these (878 and 902 cm^{-1}) correspond to the remaining 652 cm^{-1} NiTPP band, γ_{17} ($\gamma(C_\beta-H)_{sym}$), and are $\gamma(C_\beta-H)_{sym}$ vibrations centered predominantly on the pyrrolidene or pyrrole rings. Since the intensities of resonance Raman bands can be used to map the changes in geometry associated with the electronic transitions lying at the excitation wavelength, the observation that the modes which are most strongly enhanced are those which involve distortion of the C_m-pyrrole$-C_m$ segments away from their near-planar ground-state geometries may be significant. In particular, it points to distortions in the excited state along coordinates which are different to those found in the ground state. In the ground state, each of the C_m-pyrrole$-C_m$ units in TtBP is near-planar, even in this very sterically challenged compound, but the overall structure is ruffled because these units are tilted with respect to each other. However, the enhanced modes do not follow this distortion coordinate but are associated with twisting within the C_m-pyrrole$-C_m$ units and this suggests that these modes are important in the excited state.

Introduction

Nonplanar porphyrins are commonly found in biological systems and many groups have attempted to gain some insight the effects of distortion using simple model porphyrins.[1−3] The distortion from planarity in biological systems can be traced to a variety of sources, for example, bulky axial ligands and substituents around the periphery of the macrocycle give large steric interactions that can only be relieved if the porphyrin distorts from planarity. A very large number of nonplanar porphyrins have also been synthesized: in these, the distortion is induced either by introducing steric interactions using peripheral substitution or by the introduction of central metal ions of suitable size into the porphyrin core.[1,4−6]

While the perturbation of the ground-state properties of these compounds is of considerable interest, the perturbation of their excited-state properties is, if anything, more dramatic. This is important because the excited states of porphyrins are themselves intensively investigated, for example, porphyrins have already found applications in areas as diverse as molecular electronics, solar energy conversion and photodynamic therapy.[7] In many of these applications the photophysical properties of the porphyrin macrocycle are central to the functioning of the systems. In general, the nonplanar compounds have much shorter excited-state lifetimes than their planar analogues[8] and some display strongly temperature-dependent photophysical behavior.[4] This raises the possibility that the excited-state properties of the porphyrin may be "tuned" by introducing distortions into the macrocycle, but of course, such an approach requires an understanding of how the nature of the distortion is linked with the photophysical consequences.

Of the two main synthetic methods of introducing distortion into a porphyrin (metalation and substitution by sterically bulky substituents) we have chosen peripheral substitution because it allows us to study distortion effects independently of the photophysical changes which often accompany metalation. In this paper we concentrate on the free-base form of tetra-*tert*-

10.1021/jp027750a CCC: $25.00
Published on Web 03/29/2003

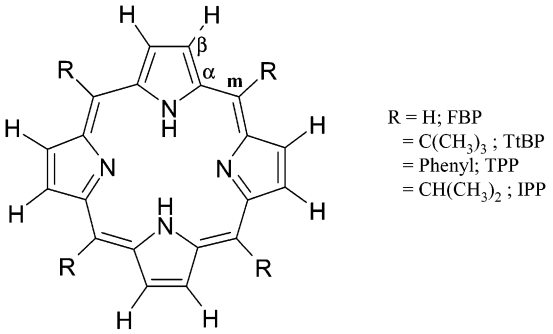

Figure 1. Structures of the various porphyrin molecules discussed in the text.

butyl porphine (TtBP), which has extremely bulky *meso* substituents, and compare it to other porphyrins, including tetraphenyl porphine (TPP) and tetra-*iso*-propyl porphine (IPP), which also have heavy but less sterically demanding substituents at the *meso* positions (see Figure 1). While it has been known for some time that free-base IPP and TPP have near-planar porphyrin cores, the crystal structure of free-base TtBP has only recently been determined. Its structure is, as expected, severely distorted from planarity with a ruffling angle of 65.5°. (The ruffling angle here is defined as the torsional angle (deg) of the C_β-C_β of opposite pyrrole rings with respect to an axis through the nitrogen atoms. Full crystal structure to be published.) As is common in nonplanar porphyrins, the Soret and Q-bands in its UV−vis spectrum are slightly shifted, although the overall spectrum is clearly that of a porphyrin.[9,10]

Raman spectroscopy is widely used in research on distorted porphyrins as it, potentially, allows the extraction of an immense amount of data on a molecular system and specifically, in the case of distorted porphyrins, it may yield information on the nonplanarity of the system. However, even if resonance Raman spectroscopy is used, so that totally symmetric vibrations are preferentially enhanced, the Raman spectra are still complex and it is very difficult to make reliable assignments of bands by analogy with the better known and understood planar porphyrins.

Recently it has been shown[11,12] that a density functional theory (DFT) approach to the calculation of the vibrational frequencies using gradient corrected functionals can perform quite satisfactorily on molecules of moderate size. As the quality of the calculations has improved, the agreement between the experimental and the calculated spectra has also improved, to the point where calculations can provide a realistic basis for making definitive assignments of the bands in experimental spectra. This improvement is due, in part, to the fact that DFT methods have provided a way of including electron correlation in the study of moderately large molecules. Although the resulting vibrational frequencies tend to be higher than those observed experimentally, they are closer to the experimental frequencies than those calculated by semiempirical and Hartree−Fock methods. The remaining overestimation of the vibrational frequencies is mainly due to neglect of anharmonicity, together with incomplete basis sets. One approach to this problem is to use DFT-SQM methods in which the calculated force constants for various bond types are scaled by standard amounts and then used to generate vibrational modes whose position is consistent with experiment. An alternative method, which is more straightforward to implement, is to use a single scaling factor for all the vibrational modes directly, although this is somewhat less effective because it does not take into account the different bonds which are involved in each of the modes. Although the determination of appropriate scaling factors for estimating experimental frequencies has received considerable attention in the literature[11,13−21] here we use a single standard value of 0.98. Similarly, although it has been shown that the intensities of resonance Raman bands can be calculated for porphyrins,[22] for our purposes we have simply used the well-established argument that Soret-excited resonance Raman spectra of porphyrins are completely dominated by totally symmetric (A) vibrational modes and we should therefore assign observed bands to calculated A modes only.

Experimental Section

The density functional calculations were performed in *Gaussian 98* using the hybrid B3-LYP functional and the 6-31G(d) basis set.[23−25] Symmetry tolerances were relaxed (IOP2/17 = 1) to give D_{2h} and D_2 symmetry for FBP and TtBP, respectively. For the calculations on TtBP, a modified GDIIS algorithm was used instead of the default rational function optimization (RFO) because the latter did not reach a stationary point under the "tight convergence" conditions used throughout this work. The standard method for calculating Raman intensities in *Gaussian 98* ("freq = Raman" keyword), which calculates intensities for plane-polarized excitation of isotropic samples, was used. Frequency and intensity data were transferred to Microsoft Excel and SPSS SigmaPlot to allow generation of traces with Gaussian line shapes and a default fwhm of 2 cm^{-1}.

Raman spectra were obtained using a conventional dispersive system that has been described previously.[26] Briefly, the spectra were recorded using 457.9 nm excitation (Spectra-Physics Ti/sapphire laser pumped by a Spectra-Physics 2020 Ar^+ laser, typically 100 mW at sample), a 180° backscattering geometry, a Jobin-Yvon HR640 single stage spectrograph, and a CCD detector. The spectra were run in KBr disks and were not corrected for detector response.

Syntheses of the free-base porphyrins were based on a modified Lindsey procedure, in which the concentrations of the reactants was increased.[9,27] Preparation of the d_8 isotopomer of TtBP followed the same synthetic route, except that pyrrole was replaced with d_5 pyrrole. The d_2 and d_{10} isotopomers were produced by dissolving d_0 and d_8 TtBP in dry THF, and then adding a few drops of deuterium oxide. The solution was then placed in a desiccator under vacuum and left until the container was dry. The central protons within the porphyrin macrocycle are slightly acidic and so can be readily exchanged for deuterons in solution.

Results and Discussion

The resonance Raman spectrum of TtBP (λ_{ex} = 457.9 nm) is compared with that of its planar (or near-planar) analogue, IPP, and a much better known and understood *meso*-substituted porphyrin, TPP, in Figure 2. It is clear that the spectra of the planar/near-planar porphyrins and the distorted TtBP share similar high-frequency bands, which in the planar compounds are known to be due to in-plane vibrations of the central porphyrin core. In contrast, in the low-frequency region, there are remarkable differences in both the band positions and intensities between planar porphyrins and TtBP.

The appearance of unusually intense low-frequency bands in the resonance Raman spectra of nonplanar porphyrins has often been noted previously.[3,22,28,29] They are believed to have similar mode compositions to the corresponding out-of-plane vibrations of planar porphyrins (which do not appear in the Soret-excited resonance Raman spectra of the planar compounds) although of course, in nonplanar porphyrins, modes cannot simply be classified as in-plane or out-of-plane, since

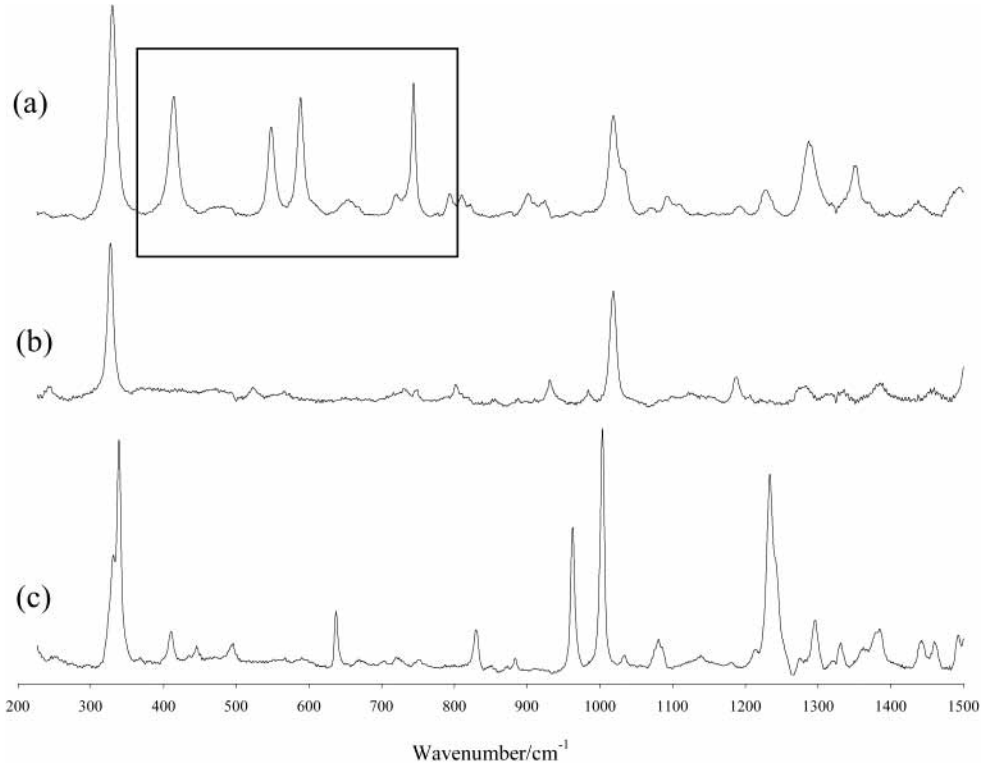

Figure 2. Resonance Raman spectra of (a) TtBP, (b) IPP, and (c) TPP, $\lambda_{ex} = 457.9$ nm. The very strong, unusual low-frequency bands of TtBP are highlighted in the box.

TABLE 1: Comparison of Experimental and Calculated Vibrational Frequency Data for FBP and Four of Its Isotopomers

FBP	d_0				d_2				d_4				d_8				d_{12}			
ν_i	exptl[a]	calcd[b]	calcd[c]	calcd[a]	exptl[a]	calcd[b]	calcd[c]	caldc[a]	exptl[a]	calcd[b]	calcd[c]	calcd[a]	exptl[a]	calcd[b]	caldc[c]	calcd[a]	exptl[a]	calcd[b]	calcd[c]	calcd[a]
ν_{l8}	155	153	160	153	155	153	155	152	155	153	161	153	153	151	158	151i	152	151	158	150
ν_8	309	304	301	304	308	303	308	302	308	304	301	303	303	298	295	298	302	298	295	297
ν_{16}	723	719	719	721	721	719	719	721	663	665	662	666	701	699	697	700	665	657	653	658
ν_7	736	724	723	728		723	721	726	702	699	697	699	722	717	715	717	699	696	695	697
ν_{15}	952	957	948	951	950	954	946	948	920	930	914	926	944	947	**767**	939	957	955	**762**	951
ν_6	987	994	985	985	978	981	968	970		962	956	957	978	980	**792**	971	923	929	**771**	924
ν_{17}	1063	1069	1055	1056	1056	1069	1055	1056	1015	1022	1007	1009	776	777	**937**	768	770	771	**921**	762
ν_9	1064	1075	1064	1062	1062	1075	1063	1061	1072	1074	1061	1061	794	799	**968**	792	773	779	**947**	770
ν_{13}	1182	1190	1178	1179	1175	1187	1175	1−177	1072	1084	1071	1071	1171	1185	1173	1175	1019	1022	1009	1010
ν_{12}	1352	1365	1352	1358		1363	1349	1356	1364	1380	1368	1318	1349	1355	1341	1347	1316	1328	1319	1316
ν_4	1400	1418	1399	1402	13601	1413	1393	1396	1330	1331	1316	1372	1401	1415	1399	1399	1359	1372	1356	1363
ν_3	1425	1450	1424	1430	1428	1449	1424	1430	1428	1443	1417	1424	1405	1426	1404	1407	1398	1420	1396	1401
ν_{11}	1492	1522	1509	1504	1496	1521	1508	1504	1485	1517	1497	1499	1450	1479	1463	1460	1451	1473	1455	1453
ν_2	1554	1574	1560	1559	1555	1574	1559	1558	1554	1571	1556	1554	1524	1545	1528	1530	1518	1539	1522	1524
ν_{10}	1609	1623	1601	1606	1614	1623	1601	1606	1601	1611	1587	1594	1615	1620	1599	1604	1598	1608	1585	1591
ν_1	3045	3136	3058	3059		3136	3058	3059		2314	2258	2258		3136	3058	2321		2314	2257	2258
ν_{14}		3190	3109	3109		3190	3109	3109		3189	3109	3109		2379	2323	2327		2379	2323	2321
ν_5	3158	3204	3124	3124	3158	3204	3124	3124		3204	3124	3124		2386	2329	3059		2386	2329	2327
ν_{NH}		3522	3367	3366		2586	2474	2474		3522	3367	3366		3522	3367	3366		3522	3367	3366

[a] Reference 34. [b] This work. [c] Reference 33.

heavily distorted porphyrins do not have a planar aromatic core. Nevertheless, the only detailed normal mode assignments of low-frequency Raman bands of nonplanar porphyrins which have been published are for NiTPP, in which weak, low-frequency bands (discussed below) can be attributed to adoption of a ruffled (S_4) geometry in solution.[30] The spectrum of TtBP (Figure 2a) displays low-frequency bands which are much more intense than those of NiTPP, which is calculated to be much less ruffled. This means that TtBP provides a model system for ruffling effects which is easier to study than is NiTPP, since the extent of ruffling and the modes associated with it are much more extreme.

Despite the fact that TtBP is a relatively large molecule and does not possess the 4-fold symmetry of many metalloporphyrins, it was possible to carry out calculations using the reasonably large 6-31G(d) basis set. The combination of this basis set with the B3LYP functional is now well-established as a useful compromise between speed and accuracy in the calculation of the vibrational spectra of medium-sized organic molecules. Since the frequencies from these calculations were then scaled using a single factor (0.98), rather than a full SQM treatment,[31] we felt it necessary to validate the approach. Simple uniform scaling has been successfully used previously and has the advantage that it avoids any ambiguities related to the choice of internal coordinate system while often giving near-comparable accuracy. The most straightforward method of validation is to use the same level of theory for free-base porphine (FBP). The previously published 6-31G(d) study of FBP also included SQM scaling, so it was not possible for us to judge the extent to which using only a single scaling factor would compromise the

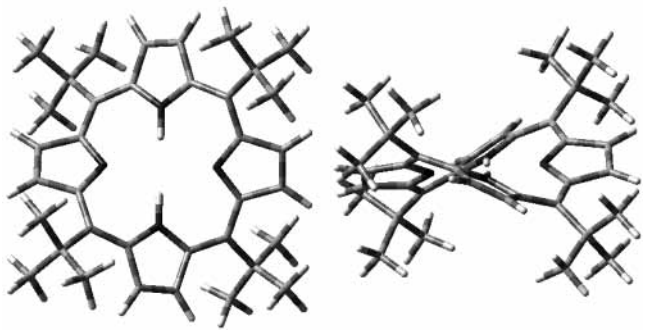

Figure 3. The calculated structure of TtBP. The molecule is highly nonplanar, with a ruffling angle of 60.8°.

accuracy of the calculated frequencies compared to a full SQM treatment. Therefore, as a first step, we carried out B3LYP/6-31G(d) calculations on FBP (D_{2h} symmetry) and several of its isotopomers (d_2, d_4, d_8, and d_{12}) and then scaled the vibrational frequencies using a 0.98 scaling factor. This was a simple way to give an indication of the accuracy that we could expect from this basis set because the resulting vibrational frequencies could be compared to experimental values[32] and to previous calculations that had employed much larger 6-31G(df,p)(5d,7f)[33] basis sets and/or SQM methods.[34] The results are shown in Table 1 and in general there is good agreement between our simple scaled frequencies and the experimental data, the errors are only slightly larger than those from SQM calculations (RMS 14.9 vs 8.4 and 10.4 cm^{-1}, respectively, for the earlier work). The only difference is that we assign the pairs of bands lying at 767, 792 and 937, 968 cm^{-1} in the d_8 isotopomer (762, 771 and 921, 947 cm^{-1} in d_{12}) differently from Tazi et al. (see bold entries in Table 1). In that work, the 767, 792 pair in d_8 were assigned as analogues of the ν_{15} and ν_6 modes which were calculated to lie at 948, 985 cm^{-1} in d_0. Similarly, the 937, 968 cm^{-1} pair were assigned ν_{17} and ν_9, which were calculated to lie at 1055 and 1064 cm^{-1} in d_0. However, visualization of these modes clearly shows that the assignment of the two pairs should be reversed so that 937, 968 cm^{-1} are ν_{15} and ν_6 while ν_{17} and ν_9 are the 767, 792 cm^{-1} pair. This revised assignment would be in agreement with other work.

Having established that simple scaling of 6-31G(d) vibrational values would ultimately give acceptably accurate frequency values, we used the same basis set and functional in calculations on free-base TtBP. Attempts to directly minimize the full molecule did not lead to the expected D_2 symmetry but gave structures very close to this point group.

Therefore the calculations were carried out on a series of input structures, beginning with a rigorously D_2 (ruffled) but unsubstituted porphyrin core, which was geometry optimized and then modified by addition of four *meso*-CH_3 groups to give a new input structure for the next stage in the calculations, which was geometry optimization of the substituted molecule. The force constants for this optimization were read from the "checkpoint" file of the parent calculation, which enabled the D_2 symmetry to be retained. Repetition of this process, adding two or four CH_3 groups in each stage, ultimately gave a full calculated TtBP

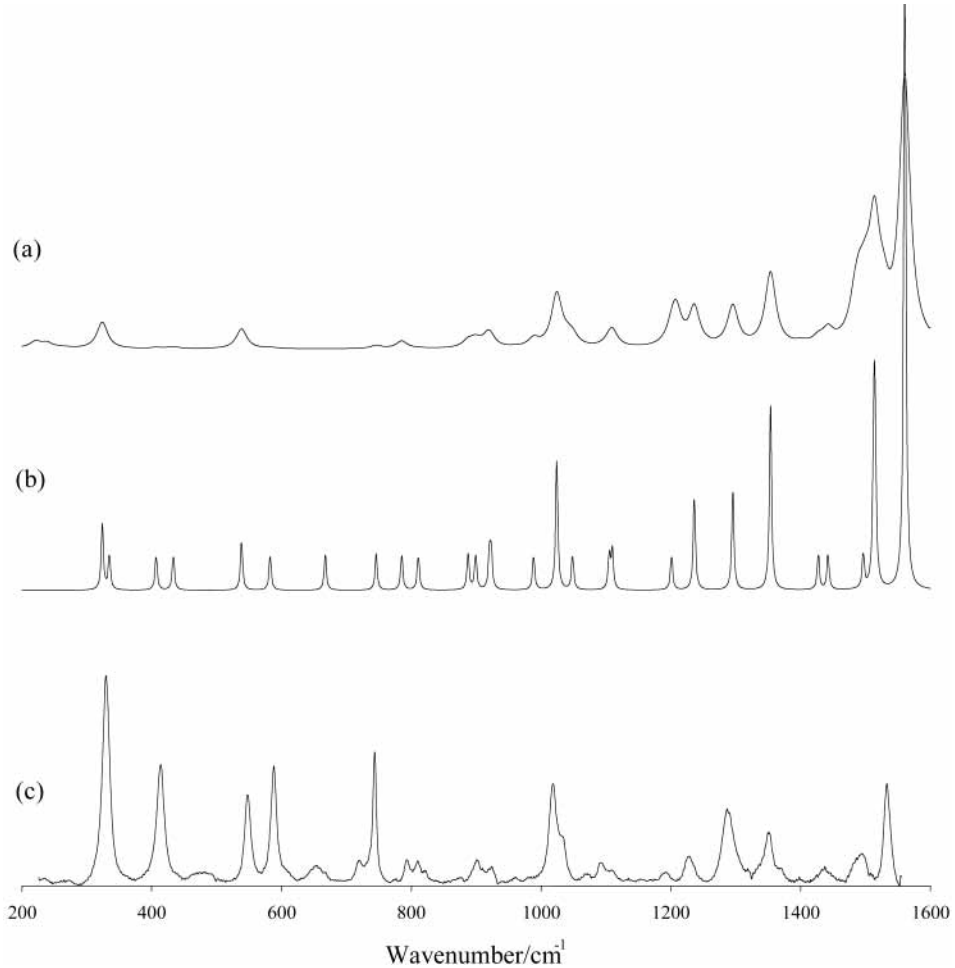

Figure 4. Calculated nonresonance trace of TtBP (a) line width = 10 cm^{-1}, intensities as per calculation and (b) line width = 2 cm^{-1}. All peaks with calculated intensity <30 A^4 amu^{-1} have been rescaled to have an intensity of 30 A^4 amu^{-1}. (c) Experimental resonance Raman spectrum of TtBP.

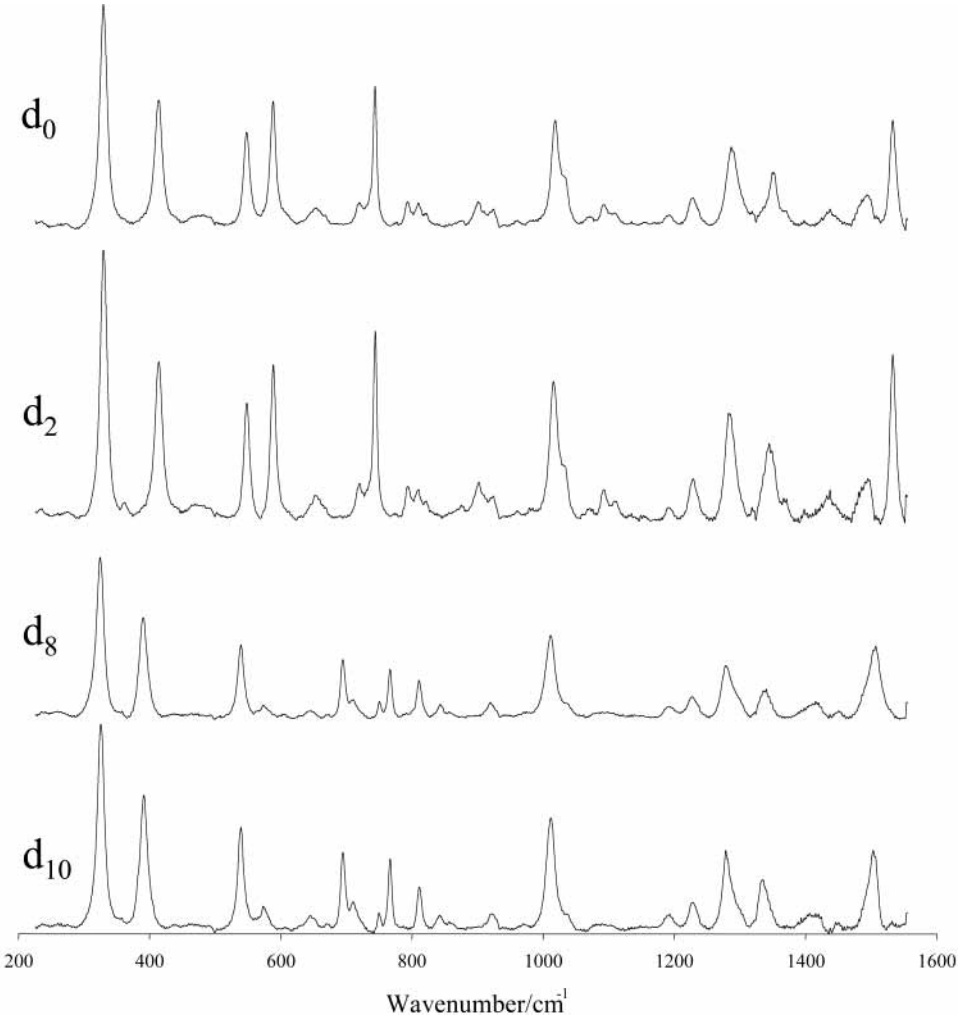

Figure 5. Resonance Raman spectra of the TtBP isotopomers in KBr, $\lambda_{ex} = 457.9$ nm.

structure with D_2 symmetry, i.e., a ruffled form. Frequency calculations on this structure gave one imaginary frequency at -8 cm^{-1}, but we feel justified in discounting this, since very low-cm^{-1} imaginary frequencies can arise in DFT calculations simply due to numerical noise. The calculated structure (see Figure 3) is very similar to the known X-ray structure, the main difference between the two is that the ruffling angle is slightly smaller in the calculated geometry (60.8° vs 65.5°).

It was important to run the calculations of the vibrational modes in a point group with the appropriate symmetry elements (rather than using a structure that was merely near-D_2) because this simplified the assignment of the large number of vibrational modes that are present. Even in D_2 symmetry, TtBP has 252 vibrational modes, 63 of which have A symmetry. Since the experimental spectra were all obtained in resonance with the Soret band, only totally symmetric A vibrations are expected to be enhanced. Of these 63 A vibrations, 22 do not fall within the spectral range investigated, 12 lie at higher cm^{-1}, since they are C−H and N−H stretches and 10 lie below 300 cm^{-1}. Finally, across the entire spectral range there are 12 vibrations of A symmetry which are composed almost entirely of motions of the ^{t}Bu substituents and which again would not be expected to appear with detectable intensity under the resonance Raman conditions used to obtain our experimental spectra since they are not associated with the chromophore.

The calculated positions and intensities of only those modes expected to be enhanced under our experimental conditions (totally symmetric modes of the porphyrin core) are shown in Figure 4a. The intensities produced by the calculation are only appropriate for nonresonance conditions while our spectra are resonance Raman spectra. This means that although several vibrational bands were calculated with very low intensity (and so cannot be easily distinguished in the simulated trace) for convenience we have simply arbitrarily redrawn the trace (Figure 4b) with a line width of 2 cm^{-1} (to help distinguish individual peaks) and rescaled all peaks with calculated intensity <30 A^4 amu^{-1} to have an intensity of 30 A^4 amu^{-1}. This makes it possible to see all 29 of the A bands which are expected to appear in this region of the resonance spectrum and is justified on the grounds that comparison between these calculated nonresonance intensities and the experimental resonance Raman spectra is effectively meaningless and the peaks in the rescaled trace are simply a visual aid for the purposes of making assignments. The calculated trace is shown here as Figure 4a because it may prove useful when experimental nonresonance spectra are available.

Comparison of the arbitrarily rescaled trace with the real spectrum (Figure 4b,c) shows that there is a good match in both the number and positions of bands. Despite this agreement we would not be confident in making assignments simply on the basis of matches between observed and calculated bands, which may possibly be coincidental, particularly since we have no good intensity information from the calculations. For this reason, we also recorded spectra and calculated band positions for three other isotopomers. The experimental resonance Raman spectra are shown as Figure 5, calculated traces (with intensities rescaled

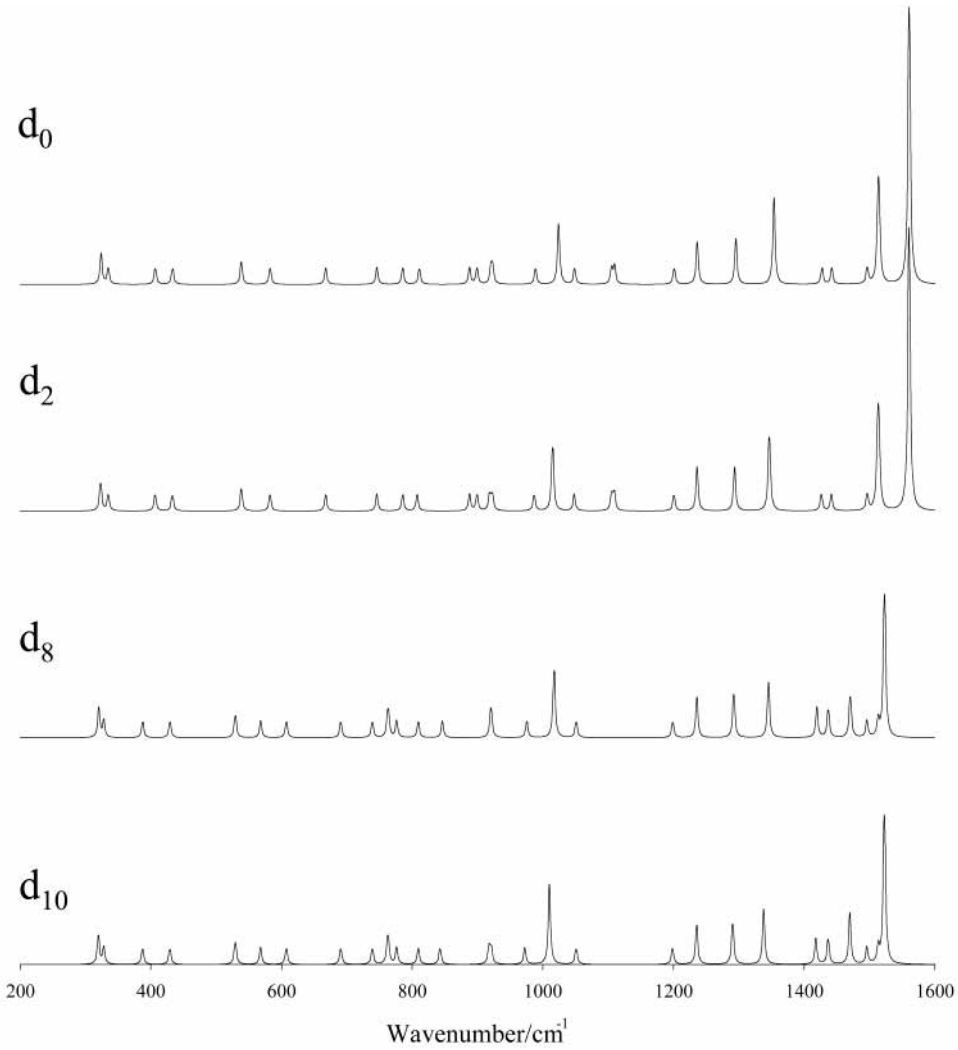

Figure 6. Calculated data for the TtBP isotopomers. In these traces the frequencies were scaled ×0.98 and intensities were arbitrarily adjusted as for Figure 4b.

as per Figure 4b) are shown in Figure 6. Table 2 brings together the observed and corresponding calculated band frequencies for all our isotopomers of TtBP. Mode labeling in the Table mostly follows that already well-established for FBP and is straightforward to derive since the vibrational motions in both compounds typically show very similar character. For some of the low-frequency ("out-of-plane") modes, the labels follow the nomenclature for NiOEP. The calculated shifts in band positions were obtained by inspection of the vibrational motions and are illustrated for the d_0/d_8 pair in Figure 7, the shifts between d_0 and d_2 and between d_8 and d_{10} are not shown because, in the main, they are too small to be distinguished in diagrams of this type (see Figures 5 and 6).

In general, the isotopomer data confirmed the assignments that could be made simply by matching the experimental bands with the closest lying calculated bands of the d_0 compound, as shown in Figure 4 above. For example, ν_4 lies as an isolated band at 1350 and 1354 cm^{-1} in the observed and calculated spectra. However, although the average deviation between calculated and observed band frequencies is reasonably small ($\sim$10 cm^{-1}) some bands would be expected to show much larger deviations (as is the case for FBP, see Table 1). This uncertainty makes assignments based on simple frequency matching between a single experimental spectrum and calculated data less convincing, which is where the isotopomer data is invaluable. For example, the highest cm^{-1} band in the experimental data for the d_0 molecule lies at 1533 cm^{-1}, we have assigned this band as ν_2, despite the fact that ν_2 is calculated at 1561 cm^{-1}. The isotopomer data confirms the assignment, with large observed (29 cm^{-1}) and calculated (38 cm^{-1}) shifts on d_8 substitution but negligible shifts on d_0-d_2 and d_8-d_{10} substitution (see Figures 5 and 6). Above 1000 cm^{-1} the observed TtBP bands are assigned to the same skeletal stretching modes that are commonly observed in planar porphyrins, such as the TPP and IPP near-analogues (see Figure 2). Indeed it is striking how little perturbation of the high-frequency skeletal modes is observed in the very highly distorted TtBP porphyrin. There are some shifts to lower cm^{-1}, as have been reported previously for a series of increasingly substituted porphyrins,[29] but the effect is not very dramatic.

The agreement between observed and calculated bands in the high-frequency region of TtBP is further evidence (along with the calculations on FBP discussed above) that the calculated frequencies obtained using a simple uniform scaling factor are sufficiently accurate to be used for mode assignments and thus they can also be used to interpret the low-frequency ($<$1000 cm^{-1}) region of the spectrum of TtBP which contains the more unusual features. As shown in Figure 2, there are several intense resonance Raman bands in the spectrum of TtBP lying in the low-frequency region. Two of these are also found in IPP and TPP and are similarly assigned here as ν_8 (ca. 330 cm^{-1}) and ν_{16} (ca. 540 cm^{-1}), although the latter band is of lower intensity

TABLE 2: Assignments of the Raman Bands of the Isotopomers of TtBP[31]

TtBP	d_0		d_2		d_8		d_{10}	
assignment	obsd	calcd	obsd	calcd	obsd	calcd	obsd	calcd
ν_8	330	324	330	323	325	320	326	320
		335		335		328		328
γ_{12}	415	407	415	407	390	387	391	387
		433		433		429		429
ν_{16}	549	538	549	538	539	529	539	529
$\gamma^{13} + \gamma_{11}$	589	583	589	583	574	568	574	568
γ_{11}	655	668	655	668	604	607	604	607
$\gamma_{11} + \gamma_{13}$	744	746	745	746	694	691	694	691
	795	785	795	785	767	776	767	776
ν_7	811	811	810	808	767	762	767	762
γ_{17} (a)	878	888	878	888	711	739	711	739
γ_{17} (b)	902	899	902	899	751	764	751	764
	925	921	925	919	920	920	920	918
	925	923	925	923	922	921	922	921
ν_{15}	1018	989	1016	987	999	975	999	972
ν_6	1031	1024	1031	1015	1012	1017	1012	1010
	1070	1049	1070	1048		1051		1051
ν_{17}	1092	1105	1092	1105	811	809	811	809
ν_9	1110	1110	1110	1109	843	846	843	843
ν_{13}	1195	1201	1195	1201	1193	1199	1193	1199
ν_1	1229	1236	1229	1236	1229	1236	1229	1236
ν_{12}	1288	1296	1284	1294	1279	1293	1279	1291
ν_4	1350	1354	1345	1347	1336	1346	1335	1338
ν_3	1438	1427	1438	1427	1420	1420	1420	1418
		1443		1442		1437		1437
ν_{10}	1494	1497	1495	1497	1491	1496	1491	1496
ν_{11}	1501	1513	1501	1513	1450	1471	1450	1470
		1515		1515		1513		1513
ν_2	1533	1561	1533	1561	1507	1523	1503	1523

in both IPP and TPP than in TtBP. This leaves three very strong bands in the spectrum for TtBP < 1000 cm^{-1} that need to be assigned, along with several other weaker features.

Assignments of unusual, but still relatively weak, low-frequency bands of NiTPP have been published and convincingly attributed to adoption of a ruffled (S_4) geometry in solution.[30] The assigned modes were named according to the scheme published for NiOEP[28] where the "out-of-plane" bands observed at 330, 547, 652, and 737 cm^{-1} were assigned to bands calculated (B3LYP/6-31G(d), SQM) to lie at 327 γ_{12}(pyr swivel), 542 $\gamma_{13}(\gamma(C_\alpha-C_m))$, 652 $\gamma_{17}(\gamma(C_\beta-H)_{sym})$, and 732 cm^{-1} γ_{11}(pyr $fold_{asym}$), respectively.

In contrast to the NiTPP case, the three strongest low-frequency TtBP bands that are "unusual" (i.e., not the skeletal stretches that are observed for all porphyrins) are very intense. The assignment of these bands is relatively straightforward since there are few bands of correct symmetry predicted to lie near them. The lowest cm^{-1} band, which is observed at 415 cm^{-1} in the d_0 compound, is assigned as γ_{12} (pyr swivel) on the basis of the calculated band position (407 cm^{-1}) and isotope shifts (see Table 2). This is one of the weak bands reported for S_4 NiTPP (obsd 330, calcd 327 cm^{-1}).

The next band, observed at 589 cm^{-1} in the d_0 compound, is assigned as a mode whose composition is a mixture of modes previously labeled γ_{13} ($\gamma(C_mC_aH_mC_a)$) and γ_{11}(pyr $fold_{asym}$) in NiOEP. This band has high intensity in both the natural abundance and d_2 spectra but only a very low intensity (at 574 cm^{-1}) in the d_8 and d_{10} isotopomers. Our calculations predict *A* bands at 583 and 568 cm^{-1} in the d_0/d_2 and d_8/d_{10} isotopomers (exactly the same cm^{-1} shift as that observed) but they all have comparable intensity. Although absolute Raman intensities are not well predicted using B3LYP/631G(d), relative intensities can provide useful information. If a dramatic change in the intensity of a band is observed in the real spectra, then there would also be a change in the predicted intensity. It is possible that the high intensity of the 589 cm^{-1} band in d_0/d_2 is the result of Fermi resonance. Our calculations support this, since the combination of two predicted *A* bands, at 270 and 324 cm^{-1}, gives 594 cm^{-1}, near-coincident with the fundamental mode at 583 cm^{-1}. However, on d_8 and d_{10} isotopic substitution, these bands shift to 267 and 320 cm^{-1}, giving a combination band at 587, which would not be in resonance with the shifted fundamental mode now lying at 568 cm^{-1}.

The final high-intensity, low-frequency band in the TtBP spectrum is observed at 744 cm^{-1} and can be assigned to a mode (calcd 746 cm^{-1}) whose composition is a mixture of modes previously labeled γ_{11}(pyr $fold_{asym}$) and γ_{13} ($\gamma(C_mC_aH_mC_a)$) in NiOEP. In this case the γ_{11} character predominates rather than γ_{13} , which predominates in the 589 cm^{-1} band.

In essence, the three strong TtBP bands have similar character and position to three of the four porphyrin ring-based, weak bands that are also observed in NiTPP. In addition there are several weaker bands in the TtBP spectra that are also 'out-of-plane' vibrations. Two of these (878 and 902 cm^{-1}) are a pair of vibrations (split by symmetry) that correspond to the remaining 652 cm^{-1} NiTPP band, γ_{17} ($\gamma(C_\beta-H)_{sym}$). They are assigned as $\gamma(C_\beta-H)_{sym}$ vibrations which are centered predominantly on either the pyrrolidene or pyrrole rings. Finally, γ_{11} lies at 655 cm^{-1}. Figure 8 shows, schematically, the displacements of the atoms for all six of the "γ" modes assigned here.

The intensities of resonance Raman bands can be used to map the changes in geometry associated with the electronic transitions lying at the excitation wavelength. In this case the excitation was within the Soret band, so it is the S_0-S_2 transition that is probed. (Strictly speaking, transitions in the Q-band region are to the S_1 state in D_4 porphyrins, and to a pair of close lying Q_x, Q_y states in the lower D_2 symmetry discussed here. This means that the Soret band should formally be labeled as S_3 or higher, but we have retained the S_2 nomenclature for the Soret state for the sake of clarity.) The observation that the modes which are most strongly enhanced are those which involve distortion of the C_m-pyrrole$-C_m$ segments away from their near-planar ground-state geometries may be significant because it points to distortions in the excited state along coordinates which are different to those found in the ground state. In the ground state each of the C_m-pyrrole$-C_m$ units in TtBP is near-planar, even in this very sterically challenged compound, but the overall structure is ruffled because these units are tilted with respect to each other. However, the enhanced modes do not follow this distortion coordinate but are associated with twisting within the C_m-pyrrole$-C_m$ units. In theory it would be possible to determine if excitation also gives further distortion along the ruffling coordinate by looking for enhancement of the ruffling mode. Unfortunately, this mode, γ_{14}, normally lies well below our spectral window. In NiP it lies at 17 cm^{-1} and the same mode is calculated here for TtBP at 32 cm^{-1}. Nonetheless, the observation of enhancement of modes which involve distortion of the C_m-pyrrole$-C_m$ segments suggests that these modes are important in the excited state.

It is self-evident that the change in the pattern of distortions which follow excitation must be due to a rebalancing of the electronic forces that try to maintain planarity for maximum conjugation through the π system and the steric interactions that drive the ruffling in the ground state. Since excitation to the S_2 state would be expected to give rise to an overall loss of bonding character within the porphyrin π system while the steric forces would be effectively unchanged, the excitation might be expected to lead to even greater distortion from planarity in the excited state than in the ground state. However, the distortion

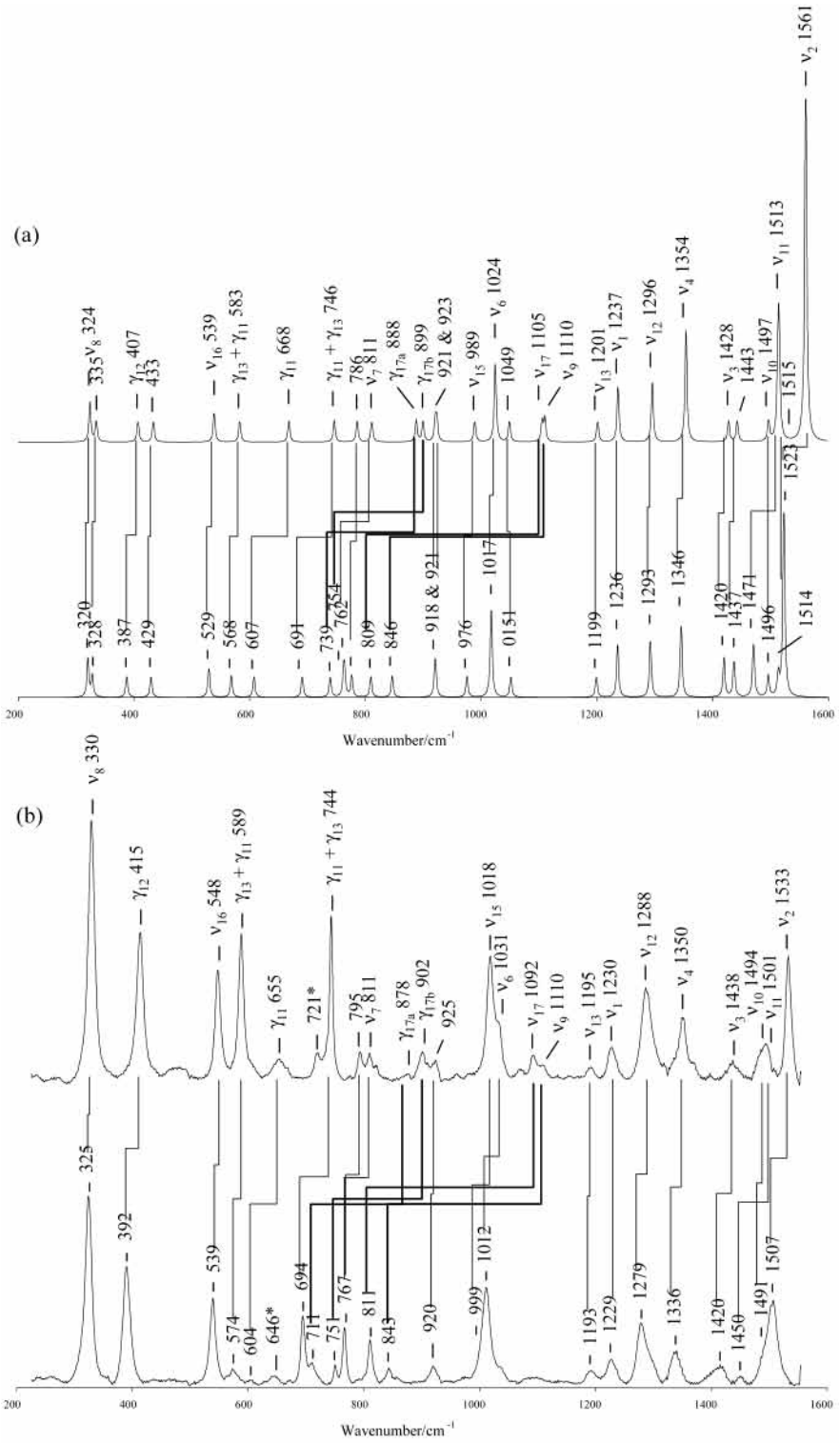

Figure 7. Calculated (a) and experimental (b) Raman spectra of d_0 (upper) and d_8 (lower) isotopomers of TtBP.

coordinate in the excited state need not necessarily follow that of the ground state. The literature on the excited states of planar porphyrins in the S_1 and T_1 clearly demonstrates that the changes in bond strength are not uniform throughout the molecules, so that while the force constants associated with some of the porphyrin ring bonds decrease on excitation, others actually increase.[35,36] These changes have been rationalized on the basis of molecular orbital calculations. Given that the redistribution of bonding is not uniform over the entire porphyrin ring it is easy to understand that the response of the ring system to the steric forces imposed by the ^{t}Bu substituents might well be different in ground and excited states and this could lead to changes in the distortion coordinate.

The observation that the intensities of the strongest low-frequency distortion modes in TtBP are very large, relative to the neighboring symmetric stretching vibrations which are common to all porphyrins, contrasts with the situation in NiTPP, in which several low-frequency vibrations have been assigned to the same modes as observed in TtBP but the bands that they give rise to are of relatively low intensity. This is presumably a result of the much weaker forces driving nonplanarity in NiTPP than in TtBP, since the smaller forces would result in a

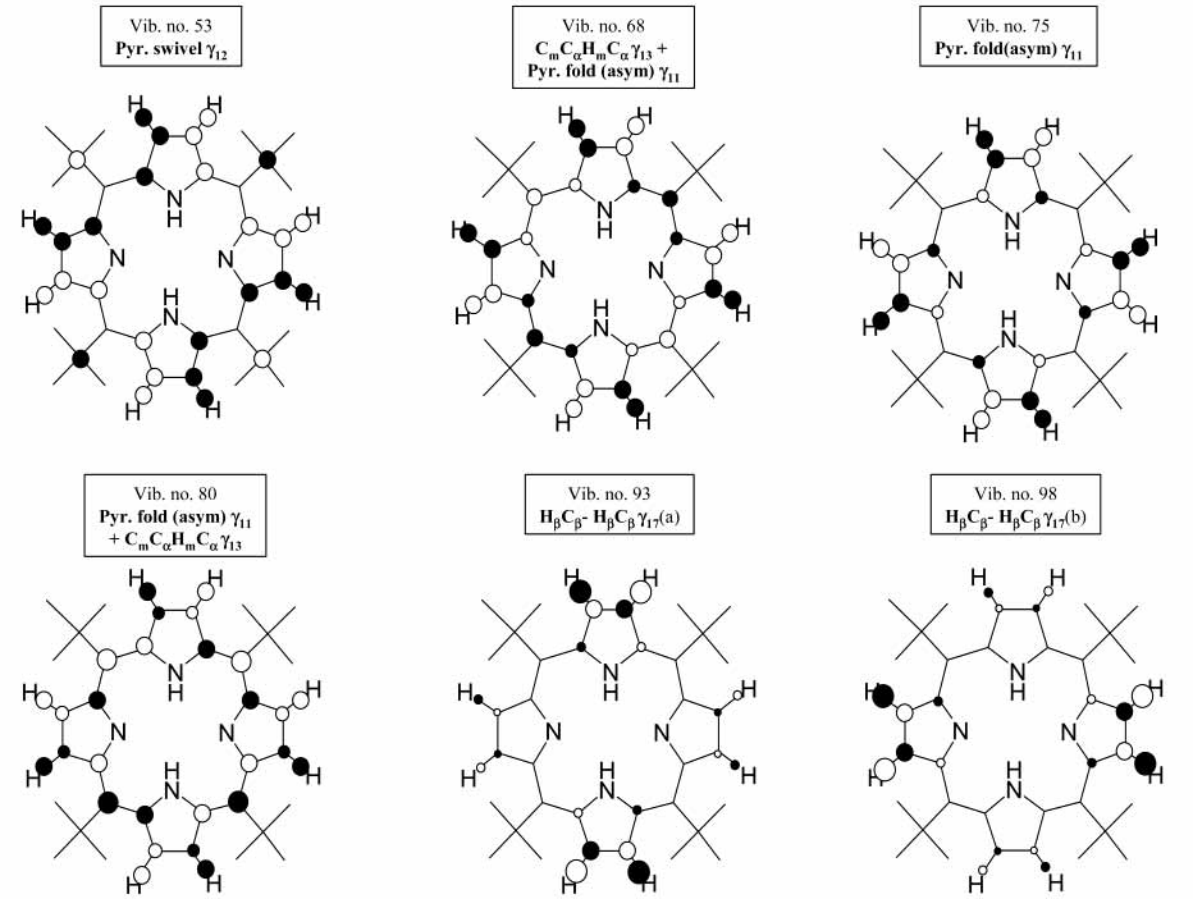

Figure 8. A schematic representation of the atomic displacements for all six of the "γ" modes of TtBP assigned in this work. The radius of the circles indicates the magnitude of the displacement, filled and open circles indicate displacement away from, or toward, the plane of the page.

smaller change in geometry along the distortion coordinates on excitation and therefore lead to lower enhancement.

Finally, the role which excited-state distortions play in modulating the photophysical properties of nonplanar porphyrins is the subject of considerable discussion in the literature. Typically, nonplanar porphyrins display markedly shorter excited-state lifetimes than planar near-analogues, for example, the S_1 lifetime of TtBP is 51 ps compared to 15 ns for TPP.[1,3,6,8] This dramatic lifetime reduction is normally attributed to conformational interconversion in the excited state, a model which has grown naturally from the observation of ready interconversion between different conformers of some nonplanar porphyrins in the ground state and the fact that in those distorted porphyrins where some luminescence can be detected, the Stokes shift is anomalously large. The results shown here, although they map the S_2 rather than the S_1 state, suggest that the conformers accessed in the excited-state manifold need not be generated by more extreme excursions along the same distortion coordinates that are followed in the ground state, but may actually involve changes in structure that are along entirely different coordinates from those which give rise to the distortion from planarity in the ground state.

Conclusion

Despite its highly ruffled structure, the high-frequency region of the resonance Raman spectrum of TtBP is similar to that of normal planar porphyrins with heavy *meso*-substituents. Similarly, its UV−vis spectrum is recognizably that of a porphyrin, despite small shifts in the position of the Soret and Q-bands. However, the strong distortion does have some striking consequences, most notably in its unusual photochemical behavior, which is believed to arise from the ease with which the distorted molecule can undergo conformational changes in the excited state, although the exact nature of these excursions is unspecified. In this context, the observation of several very intense low-frequency bands in the resonance Raman spectrum of TtBP is potentially significant. We have assigned these bands using a combination of DFT calculations and isotopomer data and found that they involve folding and swivelling of the pyrrole rings. This contrasts with the distortions of sterically congested porphyrins in the ground state which normally involve motions along the porphyrin ruffling, saddling, or doming coordinates.

Acknowledgment. R.E.O. would like to acknowledge the financial support of the McClay Trust (QUB) and the Crowther Fund (Open University) which enabled her to carry out this work.

References and Notes

(1) Jentzen, W.; Simpson, M. C.; Hobbs, J. D.; Song, X.; Ema, T.; Nelson, N. Y.; Medforth, C. J.; Smith, K. M.; Veyrat, M.; Mazzanti, M.; Ramasseul, R.; Marchon, J. C.; Takeuchi, T.; Goddard, W. A.; Shelnutt, J. A. *J. Am. Chem. Soc.* **1995**, *117*, 11085−11097.

(2) Ravikanth, M.; Chandrashekar, T. K. *Coord. Chem.* **1995**, *82*, 105−188.

(3) Shelnutt, J. A.; Song, X. Z.; Ma, J. G.; Jia, S. L.; Jentzen, W.; Medforth, C. J. *Chem. Soc. Rev.* **1998**, *27*, 31−41.

(4) Gentemann, S.; Nelson, N. Y.; Jaquinod, L.; Nurco, D. J.; Leung, S. H.; Medforth, C. J.; Smith, K. M.; Fajer, J.; Holten, D. *J. Phys. Chem. B* **1997**, *101*, 1247−1254.

(5) Smith, K. M. *Porphyrins and Metalloporphyrins*; Elsevier: Amsterdam, 1975.

(6) Spence, S. J. *Thesis; Some Studies of Nonplanar Porphyrins and Reproducible Surface-Enhancing Raman Media*; Queens University: Belfast, Northern Ireland, 2001.

(7) Milgrom, L. R. *The Colours of Life*, 1st ed.; Oxford University Press: New York, 1997.

(8) Gentemann, S.; Medforth, C. J.; Ema, T.; Nelson, N. Y.; Smith, K. M.; Fajer, J.; Holten, D. *Chem. Phys. Lett.* **1995**, *245*, 441−447.

(9) Ema, T.; Senge, M. O.; Nelson, N. Y.; Ogoshi, H.; Smith, K. M. *Angew. Chem., Int. Ed. Engl.* **1994**, *33*, 1879−1881.

(10) Parusel, A. B. J.; Wondimagegn, T.; Ghosh, A. *J. Am. Chem. Soc.* **2000**, *122*, 6371−6374.

(11) Rauhut, G.; Pulay, P. *J. Phys. Chem.* **1995**, *99*, 3093−3100.

(12) Scott, A. P.; Radom, L. *J. Phys. Chem.* **1996**, *100*, 16502−16513.

(13) Bauschlicher, C. W.; Partridge, H. *J. Chem. Phys.* **1995**, *103*, 1788−1791.

(14) DeFrees, D. J.; McLean, A. D. *J. Chem. Phys.* **1985**, *82*, 333−341.

(15) Finley, J. W.; Stephens, P. J. *J. Mol. Struct. THEOCHEM* **1995**, *357*, 225−235.

(16) Harris, N. J. *J. Phys. Chem.* **1995**, *99*, 14689−14699.

(17) Hout, R. F.; Levi, B. A.; Hehre, W. J. *J. Comput. Chem.* **1982**, *3*, 234−250.

(18) Palafox, M. A. *Int. J. Quantum Chem.* **2000**, *77*, 661−684.

(19) Peterson, P. E.; Abuomar, M.; Johnson, T. W.; Parham, R.; Goldin, D.; Henry, C.; Cook, A.; Dunn, K. M. *J. Phys. Chem.* **1995**, *99*, 5927−5933.

(20) Pople, J. A.; Schlegel, H. B.; Krishnan, R.; DeFrees, D. J.; Binkley, J. S.; Frish, M. J.; Whiteside, R. A.; Hout, R. F.; Hehre, W. J. *Int. J. Quantum Chem.* **1981**, *15*, 269−278.

(21) Pople, J. A.; Scott, A. P.; Wong, M. W.; Radom, L. *Isr. J. Chem.* **1993**, *33*, 345−350.

(22) Kozlowski, P. M.; Rush, T. S.; Jarecki, A. A.; Zgierski, M. Z.; Chase, B.; Piffat, C.; Ye, B.-H.; Li, X.-Y.; Pulay, P.; Spiro, T. G. *J. Phys. Chem. A* **1999**, *103*, 1357−1366.

(23) Becke, A. D. *Phys. Rev. A* **1988**, *38*, 3098−3100.

(24) Frish, M. J.; Trucks, G. W.; Schlegel, H. B.; Scuseria, G. E.; Robb, M. A.; Cheeseman, J. R.; Zakrzewski, V. G.; Montgomery, J. A.; Stratmann, R. E.; Burant, J. C.; Dapprich, S.; Millam, J. M.; D., D. A.; Kudin, K. N.; Strain, M. C.; Farkis, O.; Tomasi, J.; Barone, V.; Cossi, M.; Cammi, R.; Mennucci, B.; Pomelli, C.; Adamo, C.; Clifford, S.; Ochterski, J.; Petersson, G. A.; Ayala, P. Y.; Cui, Q.; Morokuma, K.; Malick, D. K.; Rabuck, A. D.; K., R.; Foresman, J. B.; Cioslowski, J.; Ortiz, J. V.; Stevanov, B. B.; Lui, G.; Liashenko, A.; Piskorz, P.; Komaromi, I.; Gomperts, R.; Martin, R. L.; Fox, D. J.; Keith, T.; Al-Laham, M. A.; Peng, C. Y.; Nanayakkara, A.; Gonzalez, C.; Challacombe, M.; Gill, O. M. W.; Johnson, B. G.; Chen, W.; Wong, M. W.; Andres, J. L.; Head-Gordon, M.; Replogle, E. S.; Pople, J. A. *Gaussian 98*; Gaussian, Inc.: Pittsburgh, PA, 1998.

(25) Lee, C.; Yang, W.; Parr, R. G. *Phys. Rev. B* **1988**, *37*, 785−789.

(26) Jones, D. S.; Brown, A. F.; Woolfson, A. D.; Dennis, A. C.; Matchett, L. J.; Bell, S. E. J. *J. Pharm. Sci.* **2000**, *89*, 563−571.

(27) Lindsey, J. S.; Schreiman, I. C.; Hsu, H. C.; Kearney, P. C.; Marguerettaz, A. M. *J. Org. Chem.* **1987**, *52*, 827−836.

(28) Li, X.-Y.; Czernuszewicz, R. S.; Kincaid, J. R.; Spiro, T. G. *J. Am. Chem. Soc.* **1989**, *111*, 7012−7023.

(29) Song, X. Z.; Jentzen, W.; Jaquinod, L.; Khoury, R. G.; Medforth, C. J.; Jia, S. L.; Ma, J. G.; Smith, K. M.; Shelnutt, J. A. *Inorg. Chem.* **1998**, *37*, 2117−2128.

(30) Rush, T. S.; Kozlowski, P. M.; Piffat, C.; Kumble, R.; Zgierski, M. Z.; Spiro, T. G. *J. Phys. Chem. B* **2000**, *104*, 5020−5034.

(31) Halls, M. D.; Velkovski, J.; Schlegel, H. B. *Theor. Chem. Acc.* **2001**, *105*, 413−421.

(32) Li, X.-Y.; Zgierski, M. Z. *J. Phys. Chem.* **1991**, *95*, 4268−4287.

(33) Tazi, M.; Lagant, P.; Vergoten, G. *J. Phys. Chem. A* **2000**, *104*, 618−625.

(34) Kozlowski, P. M.; Jarecki, A. A.; Pulay, P.; Li, X.-Y.; Zgierski, M. Z. *J. Phys. Chem.* **1996**, *100*, 13985−13992.

(35) Bell, S. E. J.; Aakeroy, C. B.; Alobaidi, A. H. R.; Hegarty, J. N. M.; McGarvey, J. J.; Lefley, C. R.; Moore, J. N.; Hester, R. E. *J. Chem. Soc.−Faraday Trans.* **1995**, *91*, 411−418.

(36) Bell, S. E. J.; Alobaidi, A. H. R.; Hegarty, M. J. N.; McGarvey, J. J.; Hester, R. E. *J. Phys. Chem.* **1995**, *99*, 3959−3964.